



# Variable-based Ramberg–Osgood constitutive model of power spinning bushing

Jun-sheng ZHAO<sup>1</sup>, Yuan-tong GU<sup>2</sup>, Wen-xin FAN<sup>1</sup>

1. School of Mechanical and Power Engineering, North University of China, Taiyuan 030051, China;

2. School of Chemistry, Physics and Mechanical Engineering, Queensland University of Technology,  
GPO Box 2434, Brisbane, QLD 4001, Australia

Received 20 June 2015; accepted 30 August 2015

**Abstract:** The influences of power spinning process parameters on the mechanical properties of spinning parts were analyzed with an SXD100/3–CNC numerical control power spinning machine. The unidirectional tensile tests were carried out. Based on the experimental data, a ternary quadratic regression equation was established by orthogonal experiment. The Ramberg–Osgood constitutive model of tin–bronze connecting rod bushing was obtained. Referred to the constitutive relation of macroscopic incremental, the incremental elastoplastic constitutive relation of spinning parts was deduced based on the Mises yield criterion and kinematic hardening model. The results can be applied to the elastoplastic analysis in finite element numerical simulation.

**Key words:** power spinning; connecting rod bushing; constitutive model; technical parameter; mechanical properties

## 1 Introduction

The future development direction of the vehicle power system is high power density (HPD). The high speed moving parts of HPD diesel engine work under the conditions of high pressure load and inertia load boundary, and it is required that bushings meet high bearing capacity [1]. Unlike other sliding bearings, the friction pair of piston pin and bushing has the characteristic of relative swing motion. The lubrication condition is relatively poor due to the piston pin and bushing or the method of splash lubrication. All these lead to the deterioration of the frictional wear on the surface of the bushing [2]. As an important branch of metal plastic processing, spinning has the advantages of flexibility and low cost, which is suitable for processing a variety of metal materials. So, it is a kind of economic and rapid plastic forming method for thin-wall parts of revolving body [3]. Compared with sheet metal forming process, the connecting rod bushing processed by power spinning has the advantages of good comprehensive mechanical properties, high fatigue strength and large bearing capacity. So, the power spinning process is an ideal processing technology for HPD diesel engine

connecting rod bushing [4]. Tin–bronze QSn7–0.2 not only has high fatigue strength and bearing capacity, but also has the advantages of good bearing performance such as anti-adhesion, compliance, embedded ability, corrosion resistance and abrasive resistance [5]. The microstructure of metal processed by power spinning is optimized, and thus its mechanical properties are improved, such as increment of strength index and resistivity, reduction of thermal conductivity and magnetic permeability, reduction of corrosion resistance. Meanwhile, its elongation can restore to that of metal processed with stress relieving annealing at a certain temperature before power spinning. Recently, the application of power spinning process for tin–bronze bushing has been widely concerned. The successful application of power spinning process in HPD diesel engine has played a role in bearing and anti-attrition. It is more applicable by power spinning to process the connecting rod bushing than by other processes. However, it is difficult to predict the mechanical properties of cylindrical parts after spinning in most cases in practice. And debugging process parameters are often used to meet the requirements of bushing.

Constitutive relation is the essential condition of the finite element analysis, which is the comprehensive

macro-mechanical properties reflection of material. The constitutive model of tin–bronze connecting rod bushing processed by spinning is uncertain, of which the mechanical performance varies with the spinning process parameters. At present, the methods for establishing the constitutive relation are divided into two types basically: one is establishing coupled constitutive equation from microstructure parameters like dislocation density and grain size, which is based on the deformation mechanism [6–8]. The other is based on the conclusion of regression analyzing experimental data to get the constitutive relation of material, which includes macroscopic stress and strain, and combines with the internal state parameters. A kind of explicit constitutive model is proposed to describe the flow behavior of materials with dynamic response characteristics in Refs. [9,10]. CHUN et al [11] predicted the flow stress of aluminum alloy using the back propagation algorithm.

All kinds of material deformation behavior can be described by the method of neural network [12–15]. It is necessary to write source programs of neural network, or to write the neural network toolbox interface programs of Matlab. Both are not easy to implement in the finite element program. At present, the constitutive relation of different spinning process parameters is an empirical formula usually obtained by the regression model. But the spinning process is very complicated and it is susceptible to the interference of various kinds of random factors, which make the influence of spinning process parameters on the flow stress. It is difficult to express the precise constitutive equation because many factors influence the flow stress in most cases. Based on bilinear elastoplastic stress–strain relation model, the stress–strain curve of bushing of different spinning process parameters can be described intuitively. But the curve near the yield point cannot be described accurately enough in this model [16].

Herein, concentrating on the key parameters of power spinning, reduction ratio  $\Psi_t$ , stress relieving annealing temperature  $t$  and feed ratio  $f$ , this paper establishes the ternary quadratic regression equation of elasticity modulus  $E$ , proof strength of plastic extension  $R_{p0.2}$ , tangent modulus  $E'$  and hardening exponent  $n$  by orthogonal experiment and unidirectional tensile test. The influence of power spinning process parameters on its mechanical properties was analyzed. The Ramberg–Osgood constitutive model of tin–bronze connecting rod bushing after spinning was studied. The constitutive relation equation of power spinning considering the process parameters was built based on the Mises yield criterion and kinematic hardening model, which can provide the basis of connecting rod bushing finite element numerical simulation.

## 2 Experimental

### 2.1 Orthogonal experiment design

The key parameters of power spinning process parameters are reduction ratio, feed rate, spindle speed, axial offset, wheel radius, and wheel forming angle. Among them, the reduction ratio, feed rate and heat treatment temperature affect the mechanical properties of spinning cylindrical parts [17].

According to the range of power spinning process parameters, three factors are selected in the experiment, namely reduction ratio, feed rate and heat treatment temperature, and five levels are selected for each factor. The factor values of the orthogonal experiment are listed in Table 1.

**Table 1** Factor values of orthogonal experiment

Test No.	Reduction ratio, $\Psi_t/\%$	Heat treatment temperature, $t/^\circ\text{C}$	Feed rate, $f/(\text{mm}\cdot\text{r}^{-1})$
1	24	263	0.13
2	24	263	0.46
3	24	296	0.13
4	24	296	0.46
5	44	263	0.13
6	44	263	0.46
7	44	296	0.13
8	44	296	0.46
9	22	280	0.30
10	46	280	0.30
11	34	260	0.30
12	34	300	0.30
13	34	280	0.10
14	34	280	0.50
15	34	280	0.30

### 2.2 Experimental method

Tin–bronze QSn7–0.2 was selected as the raw material. To avoid the influence of forming technology of cylindrical parts before spinning on the results, the physical and chemical tests were conducted for the raw material, and the results are listed in Table 2 and Table 3, respectively.

The tin–bronze rods were manufactured into cylindrical parts for tests. The inner diameter, outer

**Table 2** Mechanical properties of QSn7-0.2

Elastic modulus, $E/\text{GPa}$	Proof strength of plastic extension, $R_{p0.2}/\text{MPa}$	Tensile strength, $R_b/\text{MPa}$	Elongation after failure, $\delta/\%$
150.35	345.81	418.67	17

**Table 3** Main chemical composition of QSn7–0.2 (mass fraction, %)

Sn	Al	Zn	Fe	Pb	P	Cu
7.18	<0.002	<0.05	<0.001	<0.01	0.18	Bal.

diameter and height of the cylindrical parts are 42, 55 and 90 mm, respectively.

The tin–bronze cylindrical parts were processed with an SXD100/3–CNC numerical control power spinning machine. The tin–bronze connecting rod bushing parts before and after power spinning are shown in Fig. 1.

**Fig. 1** Tin–bronze connecting rod bushing parts before and after power spinning

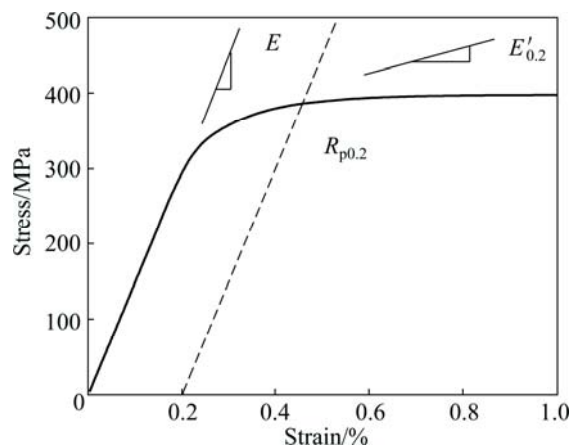
The heat treatments for cylindrical parts were carried out with a 500 kW BPG–9200BHD high temperature drying oven. All cylindrical parts were slowly heated up to 300 °C and held for 1 h, and cooled inside the furnace.

The processed cylindrical parts were machined into tensile specimens according to the tensile test method at room temperature. All specimens were loaded by microcomputer control TLS–W50000A. The testing temperature was at 20 °C, the loading rate was controlled by the displacement, and the deformation rate was 5 mm/min. A BF120–2AA strain gauge was applied to measuring the strain. Full bridge circuit was adopted to eliminate the influence of the deviation when the specimens were processed.

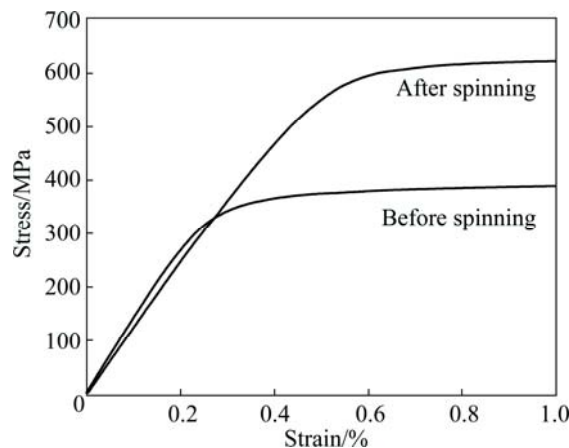
### 3 Results

Seventy five curves of force–displacement were obtained by tensile tests. After converting the force–displacement curve to the stress–strain curve, the stress–strain curve can be modified by taking the modulus of elasticity in the static tension test curve into the stress–strain curve. The main mechanical properties can be found by the graphical method, as shown in Fig. 2.

Through the tensile tests, all the stress–strain curves of specimens, elastic modulus  $E$ , yield strength  $R_{0.2}$ , tensile strength  $R_b$  and elongation  $\delta$  can be obtained.

**Fig. 2** Stress–strain curve of QSn7–0.2 in initial phase

As shown in Fig. 2,  $E$  is the elastic modulus.  $R_{p0.2}$  is the strength when the plastic elongation is 0.2%, which is known as the proof strength of plastic extension. The yield stage of QSn7–0.2 gradually changes without obvious yield point.  $E'_{0.2}$  is the tangent modulus at  $R_{p0.2}$ . Two stress–strain revised curves before and after spinning are shown in Fig. 3.

**Fig. 3** Stress–strain relationships of specimens

The value of each factor and the measured parameters, elastic modulus, yield strength, tensile strength and elongation percentage after fracture, are listed in Table 4. In order to study the change of cylindrical parts' mechanical properties before and after the heat treatments, the 16th specimen is added, which is not heat-treated. The technological parameters and measured mechanical properties of the stress–strain curves from the first to the 16th are listed in Table 4.

## 4 Ramberg–Osgood constitutive model of variable parameters

### 4.1 Elastic deformation stage

The Ramberg–Osgood model is

**Table 4** Experimental factors and main physical–mechanical properties

Test No.	Reduction ratio, $\Psi_t/\%$	Heat treatment temperature, $t/^\circ\text{C}$	Feed rate, $f/(\text{mm}\cdot\text{r}^{-1})$	Elastic modulus, $E/\text{GPa}$	Proof strength of plastic extension, $R_{p0.2}/\text{MPa}$	Tensile strength, $R_b/\text{MPa}$	Elongation after failure, $\delta/\%$
1	24	263	0.13	131.37	545	586	16.0
2	24	263	0.46	131.44	505	609	13.3
3	24	296	0.13	127.17	481	581	17.4
4	24	296	0.46	132.48	554	621	13.3
5	44	263	0.13	133.34	578	648	16.0
6	44	263	0.46	130.16	625	685	14.8
7	44	296	0.13	131.79	585	635	18.8
8	44	296	0.46	129.23	603	664	16.5
9	22	280	0.3	131.49	475	594	14.0
10	46	280	0.3	127.64	596	669	23.0
11	34	260	0.3	133.84	499	643	17.2
12	34	300	0.3	130.34	561	627	16.5
13	34	280	0.1	127.88	561	606	17.5
14	34	280	0.5	129.33	576	641	16.8
15	34	280	0.3	132.84	577	629	17.1
16	34	0	0.3	129.51	679	748	6.7

$$\varepsilon = \frac{R}{E} + \varepsilon_p \left( \frac{R}{R_p} \right)^n \quad (1)$$

The standard Ramberg–Osgood constitutive model can be used when the stress is less than  $R_{p0.2}$ . Eq. (1) can be converted into the following expression:

$$\varepsilon = \frac{R}{E} + 0.002 \left( \frac{R}{R_{p0.2}} \right)^n, \quad R \leq R_{p0.2} \quad (2)$$

#### 1) Elastic modulus $E$

The regression equation of elastic modulus obtained from the regression orthogonal table is expressed as

$$y = 130.53 + 0.059x_1 - 0.9x_2 + 0.02x_3 - 0.13x_1x_2 + 1.38x_1x_3 + 0.63x_2x_3 - 0.47(x_1^2 - 0.73) + 1.22(x_2^2 - 0.73) - 1.45(x_3^2 - 0.73) \quad (3)$$

where  $x_i$  ( $i=1, 2, 3$ ) is the coded formulas.

$$x_1 = \frac{\Psi_t - 0.34}{0.1}, \quad x_2 = \frac{t - 280}{16}, \quad x_3 = \frac{f - 0.3}{0.16}$$

All the partial regression coefficients of Eq. (3) are not significant after the tests of significance. Therefore, the regression equation can be simplified as

$$E = 130.53$$

According to the variance analysis of Eq. (3), the influence of each factor to the elastic modulus is not obvious in the ranges of the power spinning process parameters. The elastic modulus,  $E$ , of QSn7–0.2 is 130.53 GPa after power spinning. But the elastic

modulus has a certain decline, about 8%, compared with that before power spinning.

Elastic modulus is a relatively stable material constant. The elastic modulus will slightly reduce after the plastic deformation, and has less change when the reduction ratio increases to a certain degree. The elastic modulus of tin–bronze after plastic deformation can be increased by the stress relieving annealing in a small range. Therefore, the elastic modulus of tin–bronze QSn7–0.2 has a decline of 8%, which is the result of mutual influence of the process of power spinning and stress relieving annealing.

#### 2) Proof strength of plastic extension $R_{p0.2}$

The regression equation of yield strength is expressed as

$$y = 597.93 + 33.72x_1 - 4.21x_2 + 16.65x_3 - 6.63x_1x_2 + 1.38x_2x_3 + 2.62x_2x_3 - 3.53(x_1^2 - 0.73) + 5.27(x_2^2 - 0.73) - 3.19(x_3^2 - 0.73) \quad (4)$$

Taking the coded formulas into Eq. (4), we get the regression equation of proof strength of plastic extension

$$R_{p0.2} = 131.61 + 1496.60\Psi_t + 1.15t + 104.06f - 4.14\Psi_t t$$

#### 3) Hardening exponent $n$

The expression of the hardening exponent is

$$n = \frac{\ln(20)}{\ln\left(\frac{R_{p0.2}}{R_{p0.01}}\right)} \quad (5)$$

where  $R_{p0.01}$  is the proof strength when the proof strength of plastic extension is 0.01%, commonly referring to the

proportional limit.

The parameters determined by graphical and calculation method are listed in Table 5.

**Table 5** Proof strength of plastic extension  $R_{p0.01}$  and hardening exponent  $n$

Test No.	Proof strength of plastic extension, $R_{p0.01}$ /MPa	Hardening exponent, $n$
1	448	15
2	461	14
3	446	15
4	465	13
5	514	16
6	538	15
7	485	14
8	515	14
9	440	13
10	511	14
11	498	14
12	488	15
13	458	13
14	493	14
15	473	13

The regression equation of hardening exponent can be obtained from the regression orthogonal table.

$$y = 14.13 + 0.29x_1 - 0.25x_2 - 0.25x_3 - 0.25x_1x_2 + 0.25x_2x_3 + 0.25(x_1^2 - 0.73) + 0.93(x_2^2 - 0.73) + 0.25(x_3^2 - 0.73) \quad (6)$$

All the partial regression coefficients of the equation are not significant after the tests of significance. The regression equation can be simplified as constant. According to the variance analysis of regression equation, the influence of each factor to the elastic modulus is not obvious in the ranges of power spinning process parameters. There is no change of hardening exponent after spinning. The hardening exponent after rounding can be obtained to be  $n=14$ .

#### 4.2 Plastic deformation stage

As shown in the stress–strain curves of QSn7–0.2, the curves when the stress is between  $R_m$  and  $R_{p0.2}$  are similar to those when the stress is less than  $R_{p0.2}$ .  $R_m$  is the strength when the force is the maximum. Therefore, the curve can be represented by the Ramberg–Osgood model between  $R_m$  and  $R_{p0.2}$ . When the stress is larger than  $R_{p0.2}$ , the coordination of the Ramberg–Osgood expression should be translated from the origin point to  $R_{p0.2}$ , which is expressed as

$$\varepsilon' = \frac{R'}{E'_{0.2}} + A \left( \frac{R'}{R'_p} \right)^m, \quad R_{p0.2} < R \leq R_m \quad (7)$$

where  $\varepsilon'$  and  $R'$  are the strain and stress after linear

conversion, respectively.  $R'_p$  is the reference stress after conversion. Their expressions are

$$\varepsilon' = \varepsilon - \varepsilon_{0.2} \quad (8)$$

$$R' = R - R_{p0.2} \quad (9)$$

$$R'_p = R_m - R_{p0.2} \quad (10)$$

Based on Eqs. (8)–(10), we can get

$$\varepsilon - \varepsilon_{0.2} = \frac{R - R_{p0.2}}{E'_{0.2}} + A \left( \frac{R - R_{p0.2}}{R_m - R_{p0.2}} \right)^a, \quad R \geq R_{p0.2} \quad (11)$$

$E'_{0.2}$  can be expressed as

$$E'_{0.2} = \frac{E}{1 + 0.002 \frac{n}{e}} \quad (12)$$

where  $e$  is non-dimensional and can be expressed as

$$e = \frac{R_{p0.2}}{E} \quad (13)$$

Substituting the point  $(\varepsilon_m, R_m)$  into Eq. (11), the residual strain  $A$  can be expressed as

$$A = \varepsilon_m - \varepsilon_{0.2} - \frac{R_m - R_{0.2}}{E'_{0.2}} \quad (14)$$

where  $a$  is a shape index whose value is determined by a stress point between  $R_{p0.2}$  and  $R_m$ .  $\varepsilon_m$  is the strain which corresponds to the maximum pulling force.

Firstly, the curve shapes of the model are analyzed when  $a$  takes different values. When  $a$  is zero and the stress is larger than  $R_{p0.2}$ , the stress–strain curve is a straight line, whose slope is  $E'_{0.2}$ . But it does not pass through the stress point  $(R_{p0.2}, \varepsilon_{0.2})$ , which does not make sense. When  $a$  is between zero and one and the stress is larger than  $R_{p0.2}$ , the stress–strain curve is a straight line, whose slope gradually increases. This is not in conformity with the stress–strain curve of QSn7–0.2. When  $a$  is one and the stress is larger than  $R_{p0.2}$ , the stress–strain curve is a straight line connecting  $(R_{p0.2}, \varepsilon_{0.2})$  and  $(R_m, \varepsilon_m)$ , and the slope of the stress–strain curve decreases with the increase of stress. This is in conformity with the stress–strain relationship of plastic stage of bilinear model. Therefore, when  $a$  is one or larger than one, the curve of model is in conformity with the stress–strain curve.

In this work, the authors select  $R_{p0.2}$  as a reference point to determine the value of  $a$ . Its expression is shown as

$$a = \frac{\ln \left( 0.018 + \frac{R_{p2.0} - R_{p0.2}}{E} - \frac{R_{p2.0} - R_{p0.2}}{E'_{0.2}} \right) - \ln A}{\ln(R_{p2.0} - R_{p0.2}) - \ln(R_m - R_{p0.2})} \quad (15)$$

where  $R_{p2.0}$  is the stress when the plastic extensibility is 2%.

The regression equation of  $R_m$  is obtained by the regression orthogonal table:

$$y = 629.20 + 29.77x_1 - 4.24x_2 + 15.66x_3 - 5.13x_1x_2 + 0.38x_1x_3 + 1.13x_2x_3 - 0.79(x_1^2 - 0.73) + 3.16(x_2^2 - 0.73) - 4.62(x_3^2 - 0.73) \quad (16)$$

After the tests of significance, the regression equation can be simplified as

$$y = 629.20 + 29.77x_1 - 4.24x_2 + 15.66x_3 - 5.13x_1x_2 \quad (17)$$

Taking the coded formulas into Eq. (17), we can get the regression equation of tensile strength:

$$R_m = 267.23 + 1196.50\Psi_t + 0.82t + 97.88f - 3.21\Psi_t t \quad (18)$$

When the strain is the maximum, the strain is the total elongation  $\varepsilon_m$ , which can be expressed as

$$\varepsilon_m = 2.67 - 15\Psi_t + 0.059t - 5.31f \quad (19)$$

The regression equation of  $E'_{0.2}$  obtained from the regression orthogonal table is expressed as

$$y = 18.28 + 0.54x_1 + 0.26x_2 + 0.68x_3 - 0.083x_1x_2 - 0.23x_1x_3 + 0.10x_2x_3 - 0.56(x_1^2 - 0.73) - 0.67(x_2^2 - 0.73) - 0.56(x_3^2 - 0.73) \quad (20)$$

All the partial regression coefficients of the equation are not significant after the tests of significance. The regression equation can be simplified as constant. According to the variance analysis of regression equation, the influence of each factor to the tangent modulus  $E'_{0.2}$  at point  $R_{p0.2}$  is not obvious. Therefore, the value of the tangent modulus  $E'_{0.2}$  is 18.28 GPa. In the same way, the hardenability value  $m$  obtained by the regression orthogonal table is 4.

Based on the above calculations, the values of the parameters of Ramberg–Osgood model in the plastic stage are attained, as listed in Table 6.

### 4.3 Ramberg–Osgood constitutive model of spinning bushing based on variable parameters

Based on the expression above, we can get the model of stress–strain curve of QSn7–0.2 processed by power spinning, which can be expressed as

$$\varepsilon = \begin{cases} \frac{R}{E} + 0.002 \left( \frac{R}{R_{p0.2}} \right)^n, & R \leq R_{p0.2} \\ \frac{R - R_{p0.2}}{E'_{0.2}} + \left( \varepsilon_m - \varepsilon_{0.2} - \frac{R_m - R_{p0.2}}{E'_{0.2}} \right) \left( \frac{R - R_{p0.2}}{R_m - R_{p0.2}} \right)^m, & R > R_{p0.2} \end{cases} \quad (21)$$

where  $E=130.53$ ;  $R_{p0.2} = 131.61 + 1496.60\Psi_t + 1.15t + 104.06f - 4.14\Psi_t t$ ;  $n=14$ ;  $E'_{0.2}=18.28$ ;  $\varepsilon_m=2.67-$

**Table 6** Parameters of Ramberg–Osgood model in plastic stage

Test No.	Tangent modulus in $R_{p0.2}$ , $E'_{0.2}/\text{GPa}$	Proof strength of plastic extension, $R_{p0.2}/\text{MPa}$	Residual strain, $A/\%$	Hardenability value, $m$
1	16.04	559	13.15	4
2	17.63	593	10.14	4
3	15.97	565	14.16	4
4	19.17	606	12.17	4
5	16.90	636	10.18	4
6	18.79	675	8.15	4
7	18.36	615	12.17	4
8	19.46	653	10.20	4
9	18.28	576	14.15	4
10	19.28	655	8.14	4
11	18.92	632	10.20	4
12	18.32	613	13.18	4
13	18.91	593	13.20	4
14	18.66	627	13.17	4
15	19.55	614	12.18	4

$$15\Psi_t + 0.059t - 5.31f ; R_m=267.23+1196.50\Psi_t+0.82t+97.88f - 3.21\Psi_t t ; m=4.$$

The specimens were processed according to the following process parameters: reduction ratio of 34%, heat treatment temperature of 296 °C and feed ratio of 0.3. The stress–strain curve of tensile test and the curve of Ramberg–Osgood model are compared, as shown in Fig. 4. The results show that the stress–strain curves of Ramberg–Osgood model based on the parameters of the regression equation have a good agreement with the test data. The stress–strain curves of the spinning bushings can be predicted by the model accurately.

### 4.4 Derivation of incremental elastoplastic constitutive equation

The Mises yield criterion is similar to the experimental data for the elastoplastic metallic materials [18]. Due to the process of power spinning, the cylindrical parts present anisotropy, which will change according to the change of parameters of power spinning process. Therefore, the yield condition must satisfy the following formula in the process of plastic loading, which uses the Mises yield criterion and kinematics hardening model, refers to the constitutive relation of macroscopic incremental, and combines with the unidirectional tensile test results under the normal temperature:

$$F(R) = (R - h) \int d\varepsilon^p - R_{p0.2} = 0 \quad (22)$$

where  $h$  is the plastic modulus.

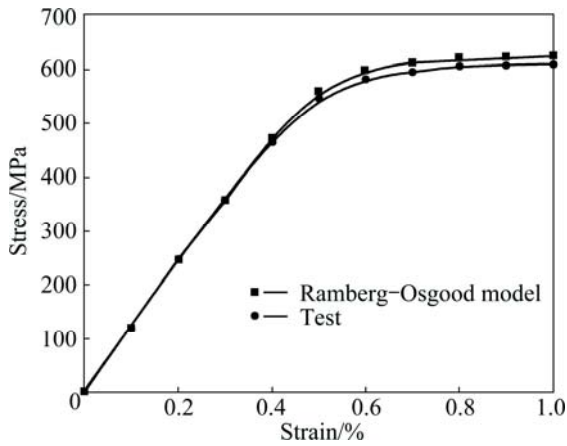


Fig. 4 Stress-strain curves of tensile test and Ramberg-Osgood model

For plastic reinforcement material, the plastic strain only appears when the stress changes from the proof strength of plastic extension. Therefore, assuming that the current stress is  $R_0$  and the current proof strength of plastic extension is  $R_{p0.2}$  in an incremental step, then the stress and strain increment are  $dR$  and  $d\varepsilon$ , respectively. The incremental constitutive equation considering the process parameters of power spinning are expressed as

$$\text{When } R_0 \leq R_{p0.2}, \quad dR = \left[ \frac{1}{E} + \varepsilon_{p0.2n} \left( \frac{R}{R_{p0.2}} \right)^{n-1} \right] d\varepsilon$$

When  $R_0 > R_{p0.2}$ ,

$$dR = \frac{d\varepsilon}{\frac{1}{E'_{0.2}} + m \left( R_m - R_{p0.2} - \frac{R_m - R_{p0.2}}{E'_{0.2}} \right) \left( \frac{R - R_{p0.2}}{R_m - R_{p0.2}} \right)^{m-1}}$$

The strain increment is usually divided into two parts. One is elasticity and the other is plasticity in the process of plastic loading:

$$d\varepsilon = \frac{dR}{E'} = \frac{dR}{E} + \frac{dR}{h} = d\varepsilon^e + d\varepsilon^p \tag{23}$$

where  $E'$  is the deformation modulus.

Therefore, in the loading incremental step, the increment of plastic strain is

$$d\varepsilon^p = \frac{dR}{h} \tag{24}$$

or

$$d\varepsilon^p = d\varepsilon - \frac{dR}{E} \tag{25}$$

By applying the constitutive Eq. (23) to the finite element analysis, the incremental method flow chart in an incremental step is shown in Fig. 5. In Fig. 5,  $R_e$  is the heuristic stress,  $R_n$  is the stress of  $n$ th iteration and  $dR^e$  is the elastic stress increment.

### 5 Conclusions

- 1) Compared with the specimens without spinning,

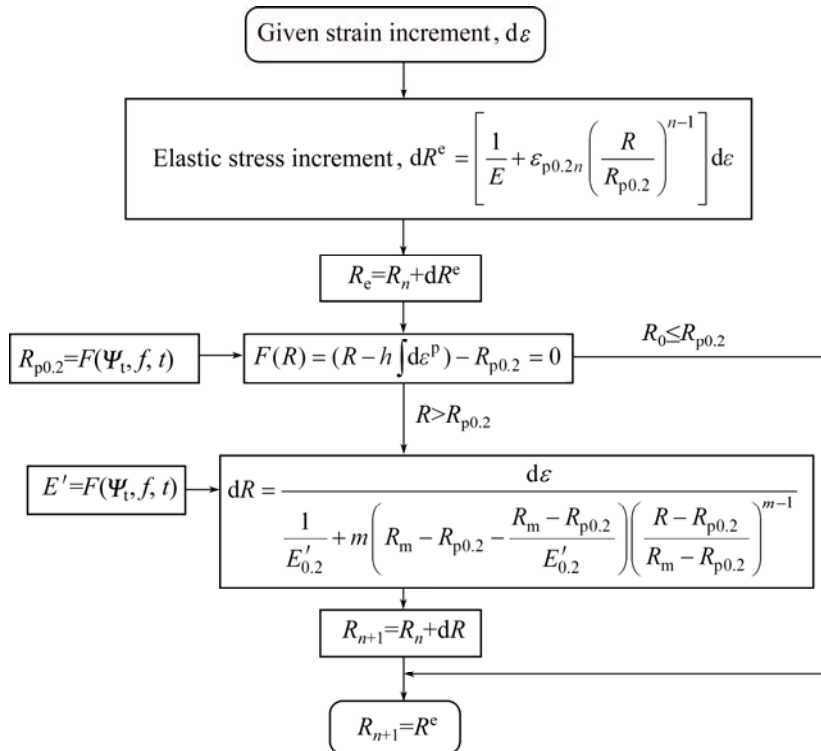


Fig. 5 Flow chart of incremental method

the elastic modulus of connecting rod bushing specimen has a decline of 8%, which maintains relatively stable. The yield strength and tensile strength have been significantly improved. The influence of reduction ratio on the strength is the most significant. The elongation drops to below 10% after spinning, which can restore to that of metal processed by stress relieving annealing at a certain temperature before power spinning.

2) Based on the parameters of reduction ratio, feed ratio and heat treatment temperature, the Ramberg–Osgood constitutive model of tin–bronze connecting rod bushing was attained, which well describes the relationship of stress–strain under different process parameters of power spinning.

3) The variable-based constitutive relation of incremental elastoplasticity of spinning parts is built based on the Mises yield criterion and kinematic hardening model, which can be applied to finite element numerical simulation.

## References

- [1] ZHAO Jun-sheng. Sliding bearing of internal combustion engines [M]. Beijing: Science Press, 2014: 15–17.
- [2] ZHAO Jun-sheng, WANG Jian-ping, YUAN Xia. Development of friction and wear testing machine on oscillation bearing [J]. Lubrication Engineering, 2014, 39(3): 101–104.
- [3] MA Fei, YANG He, ZHAN Mei. Effects of material properties on power spinning process of parts with transverse inner rib [J]. Transactions of Nonferrous Metals Society of China, 2010, 20(8): 1476–1481.
- [4] ZHAO Jun-sheng, DU Ping, FAN Wen-xin. Fretting characteristics on connecting rod bushing of diesel engine [J]. Journal of Mechanical Strength, 2015, 37(2): 209–213.
- [5] YAN Cheng-ping, WANG Li, WANG Quan-dai, XU Hua, HAO Xiu-qing, GUO Fang-liang. Tribological properties of bronze with different surface wettability [J]. Tribology, 2014, 34(3): 297–303.
- [6] JIA Bin, PENG Yan. Constitutive relationships of Nb microalloyed steel during high temperature deformation [J]. Acta Metallurgica Sinica, 2011, 47(4): 507–512.
- [7] SIAMAK S, ALI K T. An investigation into the effect of carbon on the kinetics of dynamic restoration and flow behavior of carbon steel [J]. Mechanics of Materials, 2003, 35: 653–660.
- [8] JIN Wen-cheng, ZHOU Xiao-yong, LI Na. Development of a nonlinear 3D solid finite element model for the calculation of bending moments of flexural members [J]. Academic Journal of Xi'an Jiaotong University, 2008, 20(1): 53–56.
- [9] ZHANG Chao, LI Xiao-qiang, LI Dong-sheng, JIN Chao-hai, XIAO Jun-jie. Modelization and comparison of Norton–Hoff and Arrhenius constitutive laws to predict hot tensile behavior of Ti–6Al–4V alloy [J]. Transactions of Nonferrous Metals Society of China, 2012, 22(S2): s457–s464.
- [10] WANG Zhe-jun, QIANG Hong-fu, WANG Xue-ren, WANG Guang. Constitutive model for a new kind of metastable  $\beta$  titanium alloy during hot deformation [J]. Transactions of Nonferrous Metals Society of China, 2012, 22(3): 634–641.
- [11] CHUN M S, BIGLOU J, LENARD J G. Using neural networks to predict parameters in the hot working of aluminum alloys [J]. Journal of Materials Processing Technology, 1999, 86: 245–251.
- [12] WABG Yi, SUN Zhi-chao, LI Zhi-yin. High temperature flow stress behavior of as-extruded 7050 aluminum alloy and neural network constitutive model [J]. The Chinese Journal of Nonferrous Metals, 2011, 21(11): 2880–2886. (in Chinese)
- [13] LU Shi-qiang, ZHOU Xi-lin, WANG Ke-lu. Model of constitutive relationship for 2D70 aluminum alloy based on BP neural network [J]. Forging & Stamping Technology, 2008, 33(1): 148–151.
- [14] SUN Yu, ZENG Wei-dong, WANG Shao-li. Modeling the constitutive relationship of Ti–22Al–25Nb alloy using artificial neural network [J]. Journal of Plasticity Engineering, 2009, 16(3): 126–129.
- [15] SUN Yu, ZENG Wei-dong, WANG Shao-li. Modeling of constitutive relationship of Ti600 alloy using BP artificial neural network [J]. Rare Metal Materials and Engineering, 2011, 40(2): 221–224.
- [16] LI Tao, FAN Wen-xin, ZHOU Yong-zhao. Research on constitutive relation of tube power spinning forming [J]. Hot Working Technology, 2014, 43(5): 104–106.
- [17] FENG Zhi-gang, FAN Wen-xin, ZHAO Jun-sheng. Wall thickness prediction forming of connecting rod of power spinning bushing based on BP neural network [J]. Hot Working Technology, 2014, 43(3): 129–134.
- [18] LI Yao. Technology of metal plasticity forming process [M]. Beijing: China Machine Press, 2004: 53–58. (in Chinese)

# 基于变参数的强力旋压衬套 Ramberg–Osgood 本构模型

赵俊生<sup>1</sup>, 顾元通<sup>2</sup>, 樊文欣<sup>1</sup>

1. 中北大学 机械与动力工程学院, 太原 030051;

2. School of Chemistry, Physics and Mechanical Engineering, Queensland University of Technology,  
GPO Box 2434, Brisbane, QLD 4001, Australia

**摘要:** 为了得到不同工艺参数下锡青铜衬套强力旋压后的本构模型, 采用 SXD100/3–CNC 数控强力旋压机对其进行旋压加工, 结合单向拉伸试验, 分析强力旋压工艺参数对旋压件力学性能的影响。基于获得的实验数据, 通过正交实验建立强力旋压工艺参数的三元二次回归方程, 得到锡青铜连杆衬套的 Ramberg–Osgood 本构模型。基于宏观增量本构关系, 采用 Mises 屈服准则和随动强化模型推导强力旋压的弹塑性增量本构方程。结果可用于连杆衬套的有限元弹塑性数值仿真。

**关键词:** 强力旋压; 连杆衬套; 本构模型; 工艺参数; 力学性能

(Edited by Mu-lan QIN)